Biology of Reproduction, 2018, 99(5), 949–959
doi:10.1093/biolre/ioy138
Research Article
Advance Access Publication Date: 14 June 2018

Research Article

DNA methylomes of bovine gametes and in vivo produced preimplantation embryos

Zongliang Jiang[1,†], Jianan Lin[2,3,4,†], Hong Dong[5], Xinbao Zheng[5], Sadie L. Marjani[6], Jingyue Duan[7], Zhengqing Ouyang[2,3,4,*], Jingbo Chen[5,*] and Xiuchun (Cindy) Tian[7,*]

[1]School of Animal Sciences, Louisiana State University Agricultural Center, Baton Rouge, Louisiana, USA; [2]The Jackson Laboratory for Genomic Medicine, Farmington, Connecticut, USA; [3]Department of Biomedical Engineering, University of Connecticut, Storrs, Connecticut, USA; [4]Department of Genetics and Genome Sciences and Institute for System Genomics, University of Connecticut Health Center, Farmington, Connecticut, USA; [5]Xinjiang Academy of Animal Science, Urumqi, Xinjiang, PR China; [6]Department of Biology, Central Connecticut State University, New Britain, Connecticut, USA and [7]Department of Animal Science, University of Connecticut, Storrs, Connecticut, USA

*__Correspondence:__ Xiuchun (Cindy) Tian, Ph.D., Center for Regenerative Biology, Department of Animal Science, University of Connecticut, 1390 Storrs Rd., Storrs, CT 06269, USA. Tel: 860-486-9087; E-mail: xiuchun.tian@uconn.edu; Jingbo Chen, Ph.D., Institute of Animal Science, Xinjiang Academy of Animal Science, 151 East Kalamay Street, Urumqi, Xinjiang, PR China, 830000. Tel: +86 0991-4843303; E-mail: chenjb126@126.com; Zhengqing Ouyang, Ph.D., The Jackson Laboratory for Genomic Medicine, Farmington, CT, 06032, USA. Tel: 860-837-2494; E-mail: zhengqing.ouyang@jax.org

†These authors should be regarded as joint first authors.

Edited by Dr. Sarah Kimmins, PhD, McGill University

Received 25 February 2018; Revised 6 June 2018; Accepted 12 June 2018

Abstract

DNA methylation is an important epigenetic modification that undergoes dynamic changes in mammalian embryogenesis, during which both parental genomes are reprogrammed. Despite the many immunostaining studies that have assessed global methylation, the gene-specific DNA methylation patterns in bovine preimplantation embryos are unknown. Using reduced representation bisulfite sequencing, we determined genome-scale DNA methylation of bovine sperm and individual in vivo developed oocytes and preimplantation embryos. We show that (1) the major wave of genome-wide demethylation was completed by the 8-cell stage; (2) promoter methylation was significantly and inversely correlated with gene expression at the 8-cell and blastocyst stages; (3) sperm and oocytes have numerous differentially methylated regions (DMRs)—DMRs specific for sperm were strongly enriched in long terminal repeats and rapidly lost methylation in embryos; while the oocyte-specific DMRs were more frequently localized in exons and CpG islands (CGIs) and demethylated gradually across cleavage stages; (4) DMRs were also found between in vivo and in vitro matured oocytes; and (5) differential methylation between bovine gametes was confirmed in some but not all known imprinted genes. Our data provide insights into the complex epigenetic reprogramming of bovine early embryos, which serve as an important model for human preimplantation development.

Summary Sentence

Genome-wide gene-specific DNA methylation in bovine sperm, oocytes and preimplantation embryos.

Key words: DNA methylation, gametes, preimplantation embryos, RRBS, bovine.

Introduction

Cytosine methylation is an important epigenetic modification that is largely restricted to CG dinucleotides and serves to regulate gene transcription for differentiation, gene imprinting, and X-chromosome inactivation [1–3]. The most dramatic genome-wide methylation changes occur in primordial germ cells and during preimplantation development [4–11]. In early embryos, this involves the ultimate removal of cytosine methylation acquired in the gametes prior to fertilization, a process extensively characterized at the single-base level in the mouse, and more recently in humans [4, 6–8]. Interestingly, the demethylation of the two parental genomes happens differently. Immediately after fertilization, the 5-methylcytosine (5mC) in the paternal pronucleus is actively converted to 5-hydroxymethylcytosine (5hmC) by the enzyme tet methylcytosine dioxygenase 3 (*TET3*) [12–14]. In contrast, the 5mC in the maternal pronucleus is largely protected from the actions of TET3 by *Stella/Pgc7/Dppa3*, which interacts with H3K9me2 that is enriched in the maternal pronucleus [15–17]. The differentially methylated pronuclei fuse and methylation (5mC and 5hmC) levels decrease in a replication dependent manner during cleavage division ultimately reaching a nadir. This is followed by large-scale de novo methylation that sets the stage for differentiation [18–20]. The gradual demethylation during preimplantation development has been observed in humans, mice, and cattle, but the timing of the major wave of genome-wide de novo methylation differs [4, 6–8, 18].

To date, the global characterization of the DNA methylation dynamics in embryos of domestic species remains at the immunostaining level [18, 21, 22], with the exception of a few stages of in vitro produced bovine embryos that were analyzed using the EmbryoGENE DNA methylation array [23]. These studies primarily revealed the methylation of highly condensed repetitive DNA or the methylation level of sequences represented on the array. Although numerous studies have been performed to evaluate the methylation level of selected genes and regulatory regions during bovine embryo development [21, 24–26], the complete characterization of DNA methylation at the single-base level has not been reported. This characterization is critical to understanding the epigenetic reprogramming and regulation that occurs during normal, bovine embryonic development in vivo, and to providing insight into the epigenetic alterations that occur during in vitro maturation of oocytes and culture of embryos after in vitro fertilization. Environmental perturbations experienced during in vitro production are expected to influence the epigenetic reprogramming during this critical period, often leading to nonrandom epigenetic errors [27, 28] that are linked to imprinting diseases in humans [29] and large offspring syndrome in ruminants [30, 31].

Reduced representation bisulfite sequencing (RRBS) detects clustered CGs that are mainly located in CpG islands (CGI) and are important for gene expression regulation. Here, we performed RRBS of bovine sperm, in vivo developed oocytes, and embryos from the 2-cell to the blastocyst stage, obtaining a comprehensive single-base resolution map of DNA demethylation dynamics across early bovine preimplantation development. This data resource is valuable because it provides the "gold standard" reference for embryos produced by assisted reproductive technologies, as well as identifying potential regulatory mechanisms of DNA methylation in gametes and during embryo development. Such a rich dataset from an economically important agricultural species not only provides evolutionary insights into the epigenetics of early development, but also serves as a good model for understanding potential causes of human infertility and the epigenetic effects of the assisted reproductive technologies that are designed to treat it.

Materials and methods

Ethics statement

Sperm, oocytes, and embryos were obtained from a healthy Holstein bull and cows housed at the Institute of Animal Science, Xinjiang Academy of Animal Science, Urumqi, Xinjiang, China. The animal protocol was approved by the Animal Care and Use Committee of Xinjiang Academy of Animal Science (Research license 200815).

Bovine sperm, oocytes, and preimplantation embryos

Frozen bovine sperm from a bull with proven fertility were thawed, washed, and purified to remove somatic cell contaminants using a PureCeption gradient solution. With a series dilution, approximately 50 sperm were placed into individual 0.2 ml PCR tubes and snap-frozen until analysis.

Germinal vesicle stage and in vitro matured oocytes were produced using slaughterhouse ovaries as previously described [32]. In vitro maturation was conducted in 500 μl of TCM-199 supplemented with 10% FCS and 10 ng/ml growth factor in four-well dishes for 24 h in a 39°C incubator under 5% CO_2. Maturation was confirmed by light microscopy examination and zonae pellucidae were completely removed. All oocytes were then individually snap-frozen at –80°C with minimal medium.

Multiparous Holstein cows (n = 10) were synchronized and superovulated as described previously [33]. Artificial insemination using semen from a bull with proven fertility was conducted at 12 and 24 h post standing heat (day 0). Donor animals were sacrificed at 30 h, and 2–4 days after estrus to collect in vivo matured oocytes and embryos at the 2- to 8-cell stages by oviductal flushing. Early/compact morulae and blastocysts were collected by routine nonsurgical uterine flushing on days 5, 6, and 7. All oocytes and embryos were examined and staged under light microscopy. Only morphologically intact embryos meeting the International Embryo Technology Society standards of grade 1 were included in this study.

Single oocytes and embryos were briefly washed several times in D-PBS containing 1 mg/ml polyvinylpyrrolidone (PBS-PVP). They were transferred to 50 μl droplets of 0.1% protease to remove zonae pellucidae. Single oocytes and embryos were then rinsed in PBS-PVP before assessment for the absence of contaminating cells and snap-frozen in –80°C with minimal medium. In total, we analyzed 27 individual oocytes and embryos (n = 3, per stage) and three semen samples.

RRBS library preparation and sequencing

We conducted DNA extraction, MspI digestion, end-repair, dA-tailing, adaptor ligation, and bisulfite conversion in a single tube to minimize DNA loss [34]. To monitor the rate of bisulfite conversion, 0.5% unmethylated lambda DNA (Fermentas) was spiked into all samples before MspI digestion. The converted DNA was purified with 10 ng protective carrier tRNA (Roche), followed by one round of PCR amplification with KAPA HiFi Uracil + (KAPA Biosystems). Amplified DNA fragments of 200–500 bp were size-selected using a 2% agarose gel.

RRBS libraries were prepared from three replicates of each gamete and embryo stage and multiplexed, and sequenced in Illumina

Hiseq2500 with 125 bp pair-end reads. In total, we analyzed 30 samples from 10 stages of development and obtained 165 Gb sequencing data.

Sequencing read quality control and alignment

Multiplexed sequencing reads were first trimmed to remove low-quality bases and adaptor sequences using the Trim_galore tool. The clean reads were then aligned to the bisulfite-converted reference bovine genome UMD3.1.1 (bosTau8) using Bismark alignment tools [35] (version 0.16.3) with default parameters. Additionally, because the cytosines in a non-CG (CHH and CHG) context in the lambda DNA genome are definitely unmethylated, the lambda DNA was rebuilt as an extra reference for alignment and the calculation of the bisulfite conversion rate of each sample. Once the alignment was completed, the sorted BAM files were generated by Picard toolkit and a pileup file of mapped data was created for DNA methylation calculations.

Determination of methylation levels of CpG and non-CpG sites

The methylation levels of each sampled cytosine were estimated as the number of reported C ("methylated" reads) divided by the sum of reported C ("methylated" reads) and T ("unmethylated" reads) at the same positions of the reference genome. Every CpG site with read depth >1 was summed and counted in the total CpG coverage of the sample, only the CpG sites with at least fivefold read coverage were used to quantify the DNA methylation level of each sample. We then performed the 100-bp tile-based DNA methylation calculation algorithm [6]. First, we binned the reference genome into consecutive 100-bp tiles. Then, the number of reported C divided by the sum of reported C and T captured in the 100-bp tiles was regarded as the 100-bp-tile averaged DNA methylation level. The DNA methylation level for a given sample was the average of the 100-bp tiles, while the DNA methylation level of a stage was the arithmetic average value of all biological replicates of that stage. The CpG density for every CpG site was calculated as the total number of all CpGs 50 bp up- and downstream of that CpG site. The CpG density for every 100-bp tile was calculated as the averaged CpG number in the tile. The tiles with methylation level over or equal to 20% or below 20% were defined as high/intermediate or low methylated tiles, respectively. For non-CpG methylation, the same calculation strategy was used.

Characterization of genomic features

The annotated retroelements, such as long interspersed nuclear elements (LINEs), short interspersed nuclear elements (SINEs), and long terminal repeats (LTRs), and their subfamilies were downloaded from the RepeatMasker track of UCSC genome browser. Promoters were defined as regions of 1000 bp upstream of transcription start site (TSS) of each gene. Other regions, such as CGIs, exons, and introns, were downloaded from USSC tables with UMD3.1.1 track. The intragenic regions were sequences from TSS to transcription end site (TES), while the intergenic regions were defined as the complement of intragenic regions in the bovine genome. For each annotated genomic region, the DNA methylation level was calculated from the average of all CpG sites in the region with more than fivefold coverage. Additionally, when quantifying the DNA methylation level of promoters, only those with at least five CpG sites were retained for further analysis.

Identification of dynamically methylated tiles and gamete-specific differentially methylated regions

We systematically compared the DNA methylation levels of overlapped 100-bp tiles in each of the compared groups or consecutive stages. For example, we regarded 100-bp tiles as gamete-specific differentially methylated regions (DMRs) if the methylation levels of one type of gametes (such as the sperm) were greater than 75%, while the other type (such as MII oocytes) were less than 25%, with a Benjamini-Hochberg false discovery rate (FDR) corrected $P \leq 0.05$ from a two-sided Student *t* test. Additionally, if a 100-bp tile had absolute methylation change >40% between the compared groups with an FDR-corrected Fisher's exact test of $P \leq 0.05$, it was then classified as a changing tile, while the remaining tiles were considered stable.

The gene ontology analysis was done for the genes with DMRs using DAVID online (https://david.ncifcrf.gov) [36].

Correlation of gene expression and DNA methylation

Our previously published gene expression data from bovine in vivo MII oocytes and preimplantation embryos, GSE59186 [33], and the raw data of in vitro MII oocytes, GSE52415 [37], were pooled and aligned using Tophat2 [38] against bovine genome UMD3.1.1 (bosTau8) with default settings. Cufflinks [39] was used for quantification of FPKM values with default settings. The log2 of the gene expression levels (FPKM) of detectable genes (FPKM >0.1) and the DNA methylation levels of the promoters of each corresponding expressed gene were calculated. Finally, Spearman correlation coefficients (r) between gene expression and DNA methylation levels of promoters were calculated and plotted in R package.

Results and discussion

Genome-wide DNA demethylation in bovine preimplantation embryos

Using RRBS, we analyzed a total of 30 samples that included bovine sperm and individual in vivo matured oocytes and embryos of 10 different developmental stages (n = 3) and obtained 165 Gb of sequencing data (Supplementary Table S1). The raw FASTQ files and processed methylation calling files are available at Gene Expression Omnibus (GEO) (www.ncbi.nlm.nih.gov/geo) under the accession number GSE110400. After alignment, we removed three samples with extremely low mapping efficiency (Supplementary Table S1). The bisulfite conversion efficiency, estimated from spiked Lambda DNA, was more than 99% (Supplementary Table S1). RRBS provided the expected genomic coverage and reproducibility (Supplementary Table S1 and Supplementary Figure S1a). On average, we captured 2639,860 CpGs per stage for a total of 10X genome coverage (Supplementary Table S1). Captured CpGs were broadly spread across each chromosome (Supplementary Figure S1b). The overall DNA methylation level of each developmental stage was obtained by averaging methylated cytosines in 100-bp tiles of the reference genome. Using commonly detected tiles across all stages, the methylation could be divided into two distinct profiles (Supplementary Figure S1a and Figure 1a and b): (1) highly methylated sperm and in vivo matured oocytes and (2) cleavage-stage embryos with reduced methylation, the lowest level observed at the blastocyst stage (Figure 1a and b). These patterns are similar to those found in mice [4, 6, 40] and humans [7, 8]. Two additional profiles are also noteworthy: from the 2-/4-cell to 8-cell stage, and from the early/compact morula to the blastocyst stage (Supplementary Figure S1a). The

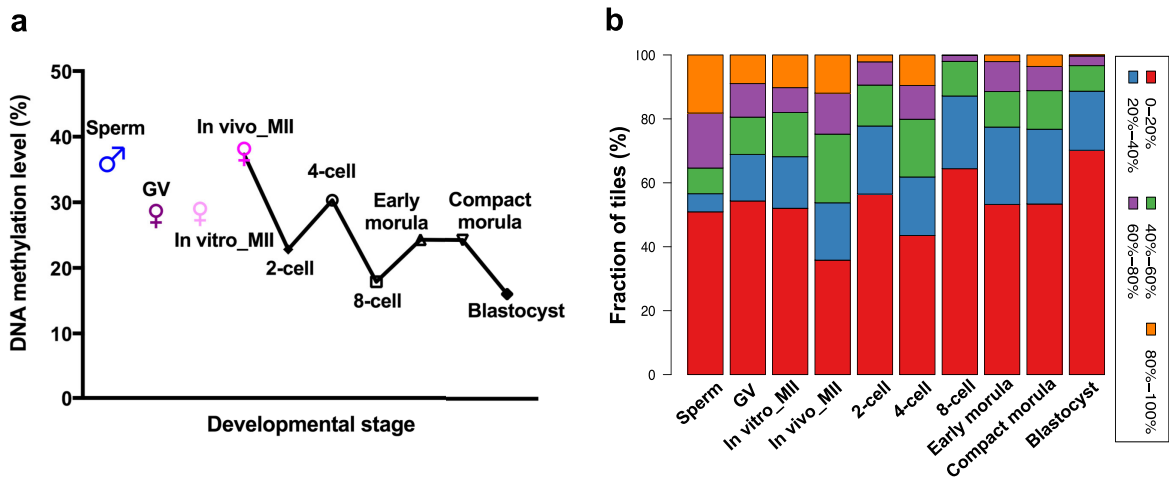

Figure 1. Bovine preimplantation embryos undergo genome-wide DNA demethylation. (a) The overall methylation levels of bovine gametes and early embryos. The averaged DNA methylation level was calculated based on the common 100-base-pair (bp) tiles detected in all stages analyzed. (b) Histogram of the fractions of tiles with 0–20%, 20–40%, 40–60%, 60–80%, and 80–100% methylation levels across different developmental stages.

demethylation during early preimplantation development has been consistently reported in 5mC immunofluorescence-based studies [18, 21, 22, 41]. However, we did not observe the de novo methylation in blastocyst stage embryos that has been observed by immunofluorescence. This could be due to several factors, chief among them the analysis of in vivo embryos in this study. In vitro production of embryos has long been known to perturb epigenetic modifications [42, 43]. Another potential cause of the discordance could be the difference in resolution between immunofluorescence and RRBS, with the former providing a localized, low-resolution view of highly methylated regions in the embryo. Lastly, it could be due to technical attributes inherent to immunofluorescence [44]. Indeed, de novo methylation at the blastocyst stage was also not observed by high-throughput sequencing analyses (RRBS or MethylC-seq) of mouse [4, 40] or human embryos [7, 8, 45].

Despite similarities to the patterns observed in mouse and human embryos, distinct features in the bovine embryos were observed. Specifically, a dramatic decrease in DNA methylation occurred between gametes and the 2-cell stage, with the average DNA methylation level decreasing from 37% in the sperm and in vivo MII oocytes to 22% in the 2-cell embryos (Figure 1a, Supplementary Figure S1c). Of interest, a significantly lower methylation level was found in the X chromosome compared to autosomes in sperm samples (Supplementary Figure S1c). A further and major reduction of DNA methylation to around 18% occurred as the embryo progressed to the 8-cell stage, coinciding with major embryonic genome activation [33, 37, 46, 47] (EGA; Figure 1a, Supplementary Figure S1c). This is consistent with the loss of methylation over multiple cleavage divisions due to the absence of the maintenance DNA methyltransferase 1 (*DNMT1*) [48], and to major increases in transcription from the embryonic genome [33, 37, 49–52]. Subsequently, an even more dramatic decrease was seen between the morula and blastocyst stages (16%; Figure 1a, Supplementary Figure S1c). The timing of this second demethylation wave correlated with the differentiation of the trophectoderm and inner cell mass, which involves the activation of specific genes, such as POU class 5 homeobox 1 (*POU5F1*) and caudal type homeobox 2 (*CDX2*) [53–55]. This is also correlated with the increased DNA methyltransferase 3 alpha (*DNMT3A*) expression in blastocysts [33]. In contrast, a moderate increase in DNA methylation was found from the 2- to 4-cell, and from 8-cell to early/compact morula, which is consistent with de novo methylation due to the elevated DNA methyltransferase 3 beta (*DNMT3B*) and *DNMT3A* expression in 4-cell and 16-cell stage bovine embryos, respectively [33]. Also of considerable interest, a significant difference in the methylation level between in vivo and in vitro matured oocytes was found (Figure 1a and b). In vitro maturation maintained GV oocyte levels of methylation while in vivo maturation increased DNA methylation levels; this is consistent with the observation that in vitro maturation produces about 75% nuclear maturation, but cytoplasmic maturation is much more incomplete [56]. As a result, in vivo-derived oocytes have a higher developmental potential compared to in vitro [32, 57]. These observations provide the underlying mechanism for the abnormal gene expression and reduced embryo and fetal development when oocytes are matured in vitro.

Genome-wide methylation maps and correlation with gene expression

As seen in mouse and human embryos [6, 7], a distinct methylation pattern was observed in and around all annotated gene bodies, which were progressively more methylated than the 15-kb intergenic regions both up- and downstream. Specifically, the TSS (or 0%; Figure 2a) was associated with a sharp decline in methylation. The methylation then gradually increased in the gene body and plateaued until another sharp decline was observed at the TES (or 100%) (Figure 2a), which brought the DNA methylation close to the level of TSS. These patterns suggest that DNA methylation may be used by cells as a unique marker for gene boundaries. Overall, promoter and CGI regions were significantly lowly methylated compared to exons and introns (Figure 2b) across all stages. This may be necessary because early bovine embryos express on average 10,000 genes [33], much higher than most differentiated tissues. Using our RNA sequencing (RNA-seq) data of early in vivo developed bovine embryos [33, 37], we found negative correlations between promoter methylation and the expression levels of corresponding genes during preimplantation development (Figure 2c), especially after EGA at the 8-cell stage and later in the blastocyst ($r<0.3$; Figure 2c, Supplementary Table S2). Because promoters, and to a large extent CGI, hardly changed their methylation levels across

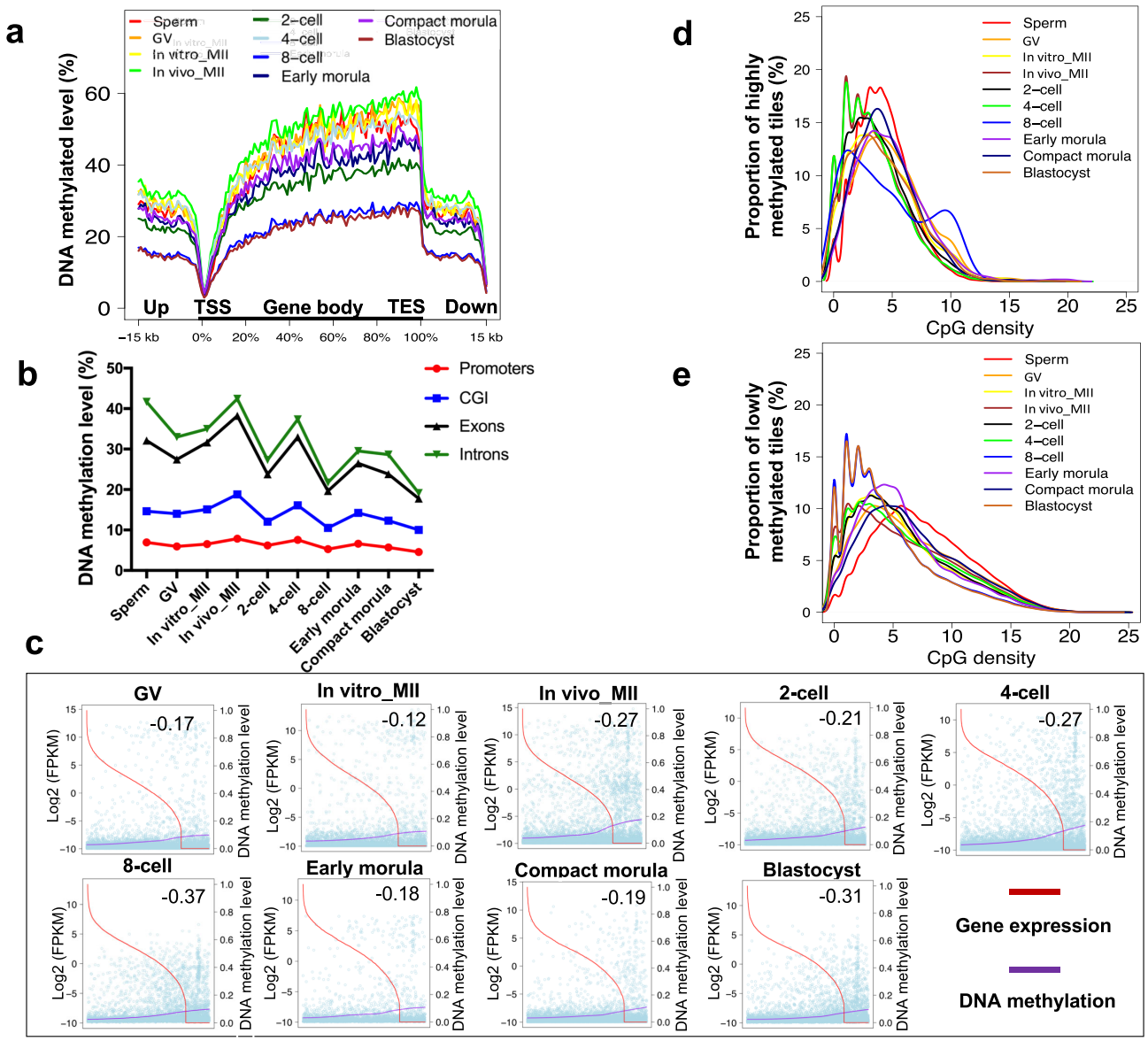

Figure 2. Characteristics of DNA methylation patterns during bovine early embryonic development. (a) Averaged DNA methylation levels along the gene bodies and 15 kilobases (kb) up- and downstream of the transcription start sites (TSS) and transcription end site (TES), respectively, of all reference genes. (b) The averaged DNA methylation level of each developmental stage on annotated bovine genome features, including promoters, CGI, exons, and introns. (c) Pearson correlation coefficients (r) of DNA methylation levels of promoter regions (purple curve) and the relative expression levels of the corresponding genes (red curve). The log2 of the gene expression levels from RNA-seq (reads per kilobase per million, RPKM) was calculated and presented. (d and e) The distribution of highly (>20%) and lowly (<20%) methylated tiles at each developmental stage against CpG density, respectively.

development, and all the methylation changes were in fact associated with exons and introns (Figure 2b), we also performed correlation analysis between CGI or exon methylation and the expression levels of corresponding genes (data not shown); similar negative correlation patterns were found with CGI or exons as in the promoter regions.

The bovine gametes and preimplantation embryos exhibited an inverse relationship between CpG density and methylation levels (Figure 2d and e); regions with high CpG density tended to be hypomethylated (<25%) and vice versa (>75%; Figure 2d and e), consistent with the patterns observed in mouse and human embryos [6, 7]. Interestingly, this correlation was more visible in gametes, and less so in the 8-cell and blastocyst stage embryos (Supplementary Figure S2), coinciding with EGA at the 8-cell stage and early lineage specification in blastocysts.

Although methylation mainly occurs at CpG sites, non-CpG methylation has been reported in oocytes [7, 58, 59] and human embryonic stem cells [60]. We also observed reduced but detectable levels of non-CpG methylation in bovine early embryos (Supplementary Figure S3a). Because RRBS detects methylation mainly in CGIs, the non-CpG methylation identified was also located within CGIs. CpG and non-CpG methylation had similar enrichment patterns in and around gene bodies (Supplementary Figure S3b); this was also observed in human oocytes [7]. Interestingly, extremely low non-CpG methylation was found in the sperm, 8-cell, and blastocyst stage embryos (Supplementary Figure S3a), all of which had

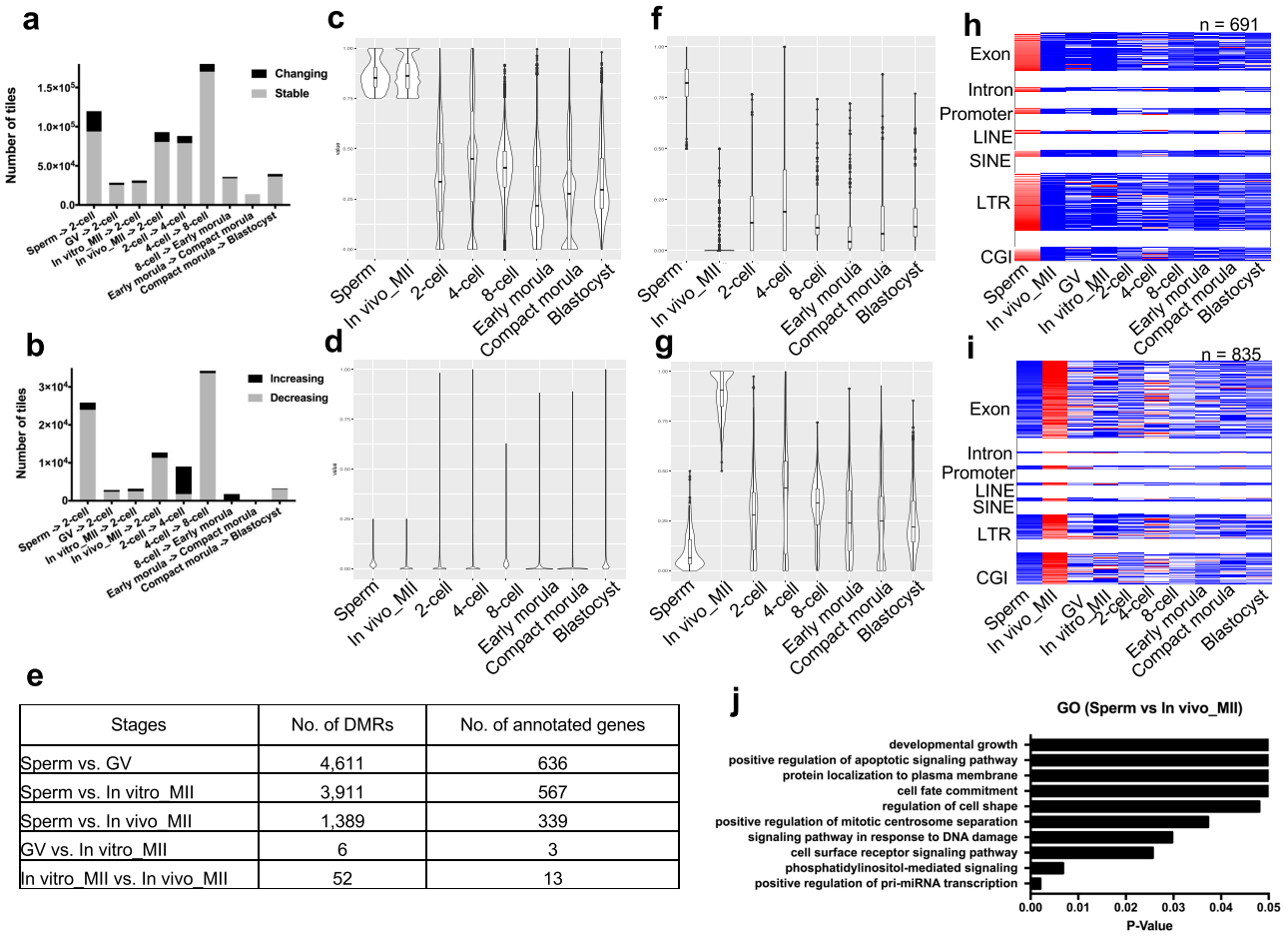

Stages	No. of DMRs	No. of annotated genes
Sperm vs. GV	4,611	636
Sperm vs. In vitro_MII	3,911	567
Sperm vs. In vivo_MII	1,389	339
GV vs. In vitro_MII	6	3
In vitro_MII vs. In vivo_MII	52	13

Figure 3. Major transitions in DNA methylation during bovine early development and key features of gamete-specific differentially methylated regions (DMRs). (a) The number of common tiles between gametes and consecutive stages that changed (black) or were stable (gray) in DNA methylation. (b) The number of common tiles between gametes and 2-cell embryos or embryos at consecutive stages of development that either had increased (black) or decreased (gray) methylation levels. DNA methylation levels in early embryos for tiles hypermethylated (c) and hypomethylated (d) in sperm and in vivo matured oocytes. (e) The number of DMRs and the number of corresponding genes between gametes of different types. DNA methylation levels of DMRs specific for sperm (f) and in vivo matured oocytes (g) in early embryos. Heatmaps of methylation levels (blue to red = low to high) for DMRs specific for sperm (h) and in vivo matured oocytes (i) in early embryos. Only DMRs that are significantly different ($P < 0.05$) between sperm and in vivo MII oocytes are presented. (j) Top represented gene ontology (GO) terms enriched in genes that had differential methylation between sperm and in vivo matured oocytes.

no enrichment in gene bodies (Supplementary Figure S3b); the low non-CpG methylation was also found in human sperm and embryos [7]. Additionally, there was no correlation between the levels of non-CpG methylation around gene bodies and expression in bovine gametes and early embryos ($r < 0.01$; Supplementary Figure S3c). It has been shown that non-CpG methylation regulates the expression of some genes (e.g. pyruvate dehydrogenase kinase 4 (*PDK4*)) [61] while not others (e.g. PPARG coactivator 1 alpha (*PGC-1α*)) [62]. Since non-CpG methylation is prevalent only in specific tissues and cell types, or only in particular regions of the genome, its functional role remains unknown [63].

Signatures of differential methylation in bovine gametes

Although the overall levels of methylation underwent dramatic changes across embryonic stages (Figure 1a), the actual numbers of tiles with changed DNA methylation between consecutive stages were only minor compared to the number of stable ones. The greatest number of changed tiles was found between gametes and early cleavage embryos, and between the 4- and 8-cell stage embryos (Figure 3a) and corresponded to the overall level changes shown in Figure 1a. These changing tiles were likely involved in the activation of gene expression from the embryonic genome at these stages as we reported previously [33]. Notably, most regions in the genome showed reduced methylation in the first wave of EGA (between MII oocytes and the 2-cell stage) and major wave of EGA (between 4- and 8-cell embryos; Figure 3b), likely from replication-dependent dilution and the lack of *DNMT1* [64]. From early morula to blastocyst stage, there was a minor increase in the number of tiles with reduced methylation (Figure 3a and b), consistent with the increase of methyltransferase expression (*DNMT3A, B*) during this transition [4, 33, 64, 65].

We next examined the similarities in DNA methylation between sperm and oocytes. Sperm and MII oocytes showed comparable methylation patterns for most covered tiles, which were either hypermethylated (methylation level ≥75%) or hypomethylated (≤25%) in both gametes (Figure 3c and d, Supplementary Figure S4a–d). The hypermethylated regions appeared gradually demethylated

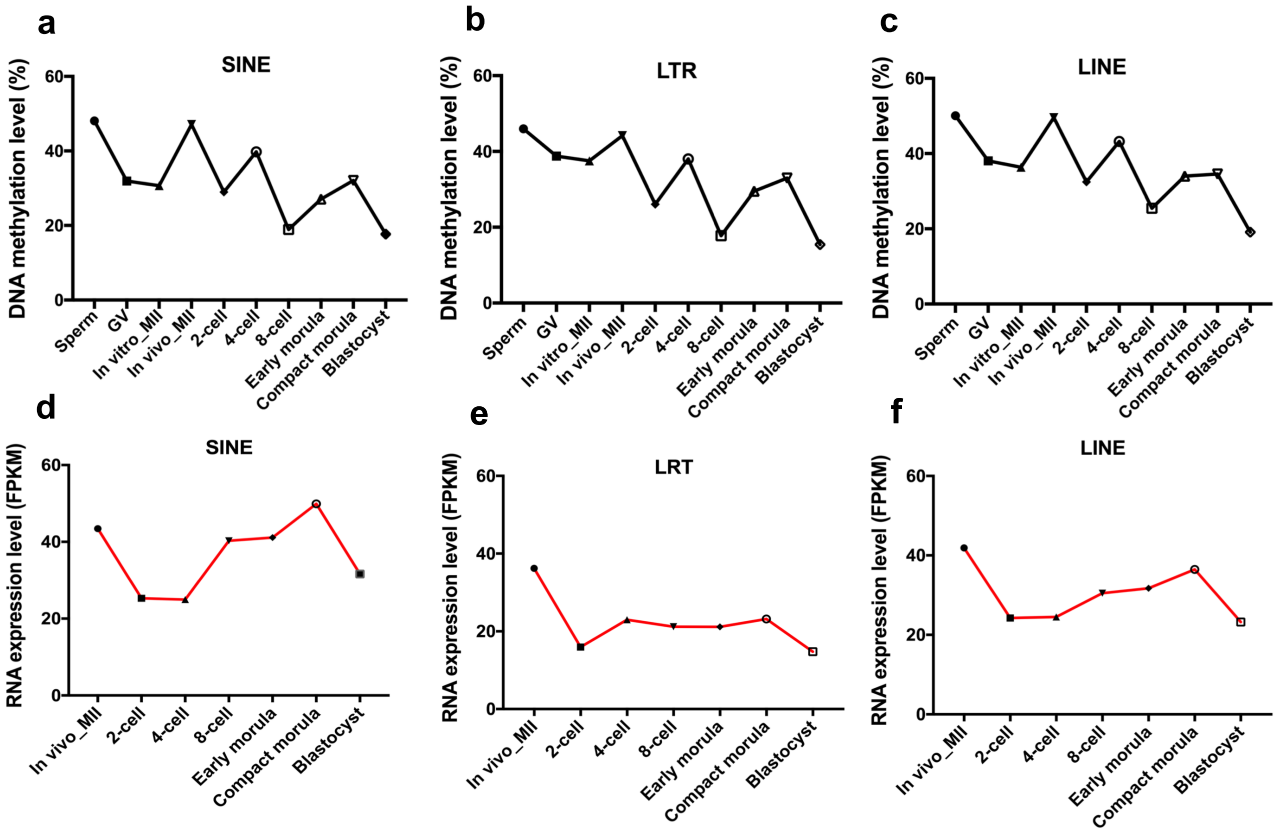

Figure 4. Dynamics of DNA methylation and expression patterns of transposable elements. DNA methylation levels of short interspersed nuclear elements (SINEs; a) long terminal repeats (LTRs; b), and long interspersed nuclear elements (LINEs; c). Relative expression levels of SINEs (d), LTRs (e), and LINEs (f).

across cleavage stages, while the hypomethylated regions remained relatively unchanged (Figure 3c and d, Supplementary Figure S4a–d). We further found that regions that were commonly hypermethylated in both sperm and oocytes were enriched in LINEs and SINEs as well as introns (Supplementary Table S3), suggesting that hypermethylated regions in bovine gametes probably mainly serve to repress the activity of transposable elements, and play a role in regulating alternative splicing [66, 67]. In contrast, commonly hypomethylated regions were enriched in promoters and CGIs (Supplementary Table S3), suggesting these regions are important for the dynamic gene activity in embryogenesis. A similar phenomenon was seen in human embryos [7].

We also examined significantly ($P < 0.05$) DMRs between sperm and oocytes. In total, we identified 1389 DMRs between sperm and oocytes matured in vivo, which corresponded to 339 genes (Figure 3e, Supplementary Table S4). Of note, sperm-specific DMRs, which were strongly enriched in LTRs (Figure 3h), rapidly lost methylation to the background level by 2-cell stage. Oocyte-specific DMRs, however, were often localized to exons and CGIs (Figure 3i) and demethylated gradually across cleavage stages (Figure 3f and g, Supplementary Figure S4g–j). Consistent with the overall averaged methylation levels (Figure 1a), both oocyte- and sperm-specific DMRs were more methylated than the same DMRs in cleavage and blastocyst stage embryos (Figure 3h and i). Gene ontology analysis showed that genes associated with gamete-specific DMRs were clearly enriched for active cellular functions, such as regulation of transcription, signaling pathway, cell shape, cell fate, and developmental growth (Figure 3j).

Because more developmental failures occur in conceptuses derived from in vitro matured oocytes than those matured in vivo [32, 68], we further investigated the differential DNA methylation between these two types of oocytes. A total of 52 DMRs ($P < 0.05$; Figure 3e, Supplementary Table S5), associated with 13 genes, were found (Figure 3e, Supplementary Table S5). Interestingly, many of them have not been characterized for their roles in maturation, making them good candidates for gene-specific epigenetic modification studies. During in vitro maturation only six tiles, corresponding to three genes (Figure 3e), carbonic anhydrase 6 (*CA6*), caspase recruitment domain family member 11 (*CARD11*), and espin like (*ESPNL*), changed their methylation from the GV stage.

Dynamics of DNA methylation and expression patterns of transposable elements

SINEs represent the majority of bovine genome repetitive content with LINEs being the second most prevalent [69]. Since we uncovered high levels of methylation of these sequences in the gametes, we were interested in determining the correlation of DNA methylation with the expression of SINEs and LINEs across development. Regardless of the sequences, the transposable elements had similar DNA methylation dynamics to what was seen for the overall genome methylation, i.e. higher methylation in sperm and in vivo matured oocytes, followed by demethylation at the 8-cell stage, reaching a nadir in blastocysts (Figure 4a–c). Transcription of all transposable elements, however, did not appear to follow the changes in DNA methylation except between the 2- and 8-cell stages (Figure 4d–f),

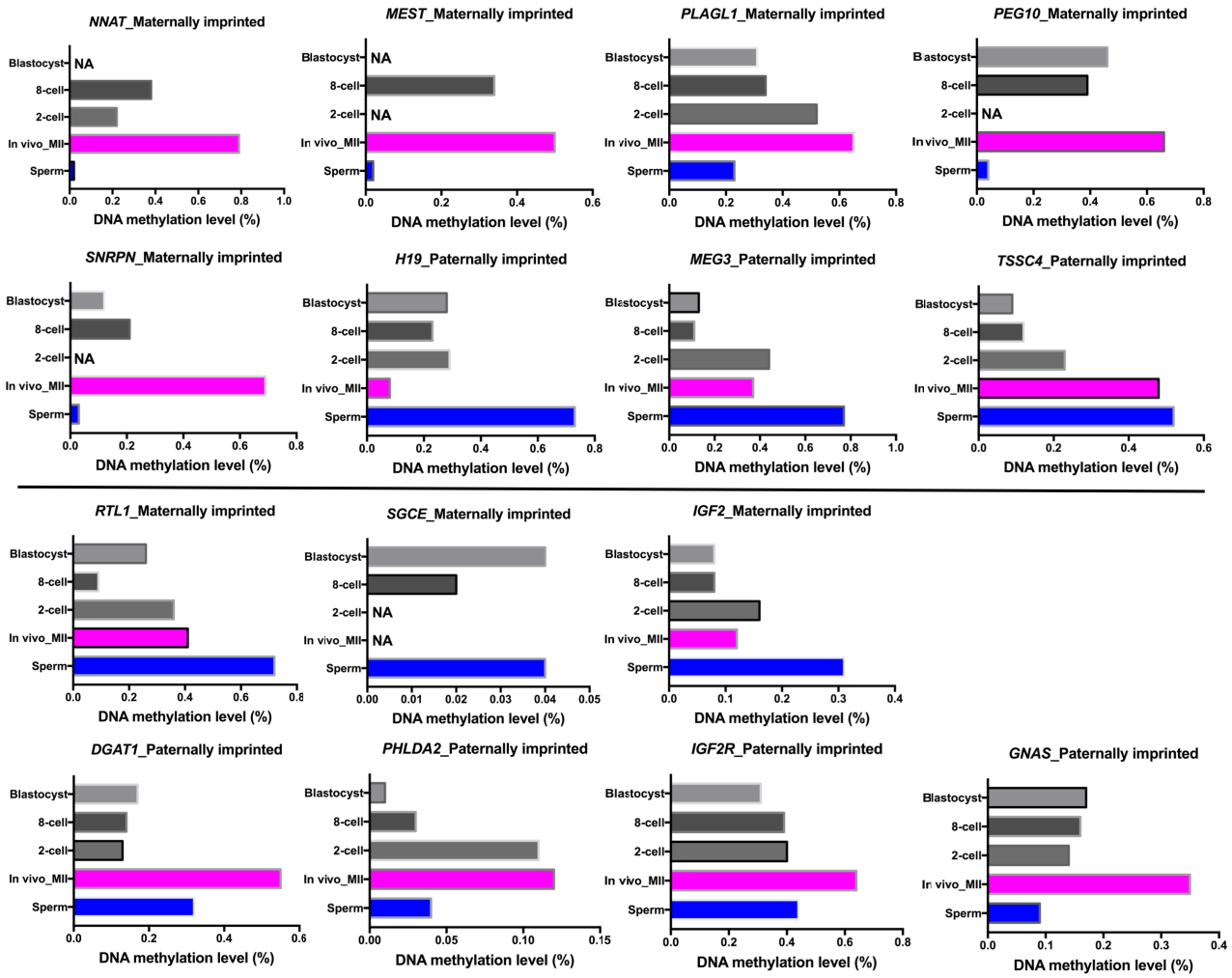

Figure 5. Methylation patterns of imprinted genes in bovine gametes. The DNA methylation levels of 15 known paternally and maternally imprinted genes in bovine gametes and early embryos. NA: methylation sites were not detected in the regions.

where there seems to be a rough negative correlation of DNA methylation and transcription levels. It is possible that other mechanisms, or methylation not revealed by RRBS, are involved. Furthermore, evolutionary age of the transposable elements appeared to be correlated with methylation levels. For example, BovB (suggested to be old) had the highest methylation levels across all stages compared to other transposable elements (Supplementary Figure S5a). However, the observation that the evolutionarily younger L1 had a slightly higher methylation and transcription levels than L2 in bovine oocytes and early embryos (Supplementary Figure S5b) may suggest that young transposable elements are not demethylated to the same extent as their older counterparts.

DNA methylation dynamics of imprinted genes in bovine gametes and embryos

The mechanism of genetic imprinting often involves allele-specific DNA methylation in oocytes and sperm [70]. To date, the DNA methylation profiles of bovine imprinted genes have not yet been well characterized in bovine gametes and across pre-implantation development, with the exception of small nuclear ribonucleoprotein polypeptide N (*SNRPN*), mesoderm specific transcript (*MEST*), PLAG1 like zinc finger 1 (*PLAGL1*), paternally expressed 10 (*PEG10*), insulin like growth factor 2 receptor (*IGF2R*), and insulin like growth factor 2 (*IGF2*) in sperm and oocytes [71, 72], and *SNRPN*, *MEST*, *PLAGL1*, *PEG10*, *IGF2*, and imprinted maternally expressed transcript (*H19*) in day 7 blastocysts [24, 73]. We assessed the methylation levels of all 29 genes known to be imprinted in the bovine (http://www.geneimprint.com/site/genes-by-species.Bos+taurus) [74–76]. Only 15 were well covered by the captured CpGs using RRBS. Five maternally imprinted genes (neuronatin (*NNAT*), *MEST*, *PLAGL1*, *PEG10*, and *SNRPN*) had higher DNA methylation in in vivo matured oocytes than sperm (Figure 5). Conversely, three paternally imprinted genes (*H19*, maternally expressed 3 (*MEG3*), and tumor-suppressing subchromosomal transferable fragment 4 (*TSSC4*)) were more methylated in the sperm (Figure 5). As expected, the methylation levels for these eight imprinted genes in cleavage stage embryos were half of the high levels observed in gametes (Figure 5). These DMRs are good candidates for further study to determine if they are imprinting control elements. Our results not only confirmed that a number of bovine imprinted genes contain allele-specific methylated regions [71, 77], but

also provide evidence that the methylation in these regions resisted the global demethylation process in early embryonic development as anticipated [78].

Interestingly, the methylation patterns of three maternally imprinted genes, retrotransposon Gag like 1 (*RTL1*), sarcoglycan epsilon (*SGCE*), and *IGF2,* and four paternally imprinted genes, diacylglycerol O-acyltransferase 1 (*DGAT1*), pleckstrin homology like domain family A member 2 (*PHLDA2*), *IGF2R*, and GNAS complex locus (*GNAS*), had the opposite methylation patterns than expected (Figure 5). It is worth noting that the levels of methylation for *SGCE* and *PHLDA2* were low (Figure 5). A previous study also reported higher methylation of *IGF2* [72] in sperm than in oocytes. In addition, most imprinted genes are clustered and controlled by imprint control regions in mice and seven of the clusters have been well characterized, including *IGF2*, *IGF2R*, and *GNAS* [79, 80]. Experiments have also indicated that the DMRs have different effects in these three clusters and suggested that knowing the position of the DMR with respect to the imprinted genes in each cluster is essential for understanding their exact regulation mechanisms [80]. Moreover, the mRNA expression of all these genes, except for *GNAS,* was extremely low in bovine gametes and early embryos [76]; therefore, it is likely that the imprinting regulation of such genes involves other epigenetic mechanisms [76, 81].

Supplementary data

Supplementary data are available at *BIOLRE* online.

Supplementary Figure S1. (a) Pearson correlation heatmap of DNA methylomes. GV: germinal vesicle stage oocytes; in vitro_MII: MII oocytes matured in vitro; in vivo_MII: MII oocytes matured in vivo. The numbers attached to the sample names indicate biological replicates. The color from blue to red indicates the correlation coefficient of low to high. (b) Histograms of the numbers of 100-base-pair (bp) CpG tiles captured on each chromosome across developmental stages. (c) Histograms of the average methylation levels of the 100-base-pair (bp) CpG tiles captured on each chromosome across developmental stages.

Supplementary Figure S2. Box plots of methylation levels at each stage across local CpG densities.

Supplementary Figure S3. (a) The non-CpG methylation levels across each stage of bovine gametes and early embryos. The averaged non-CpG DNA methylation level of each developmental stage is calculated based on the overlapped 100-base-pair (bp) tiles detected in all of the developmental stages analyzed. (b) The averaged non-CpG DNA methylation levels along the gene bodies and 15 kilobases (kb) upstream of the transcription start sites (TSS) and 15 kb downstream of the transcription end site (TES) of all reference genes. (c) Scatter plots of non-CpG DNA methylation levels of gene body regions and the relative expression levels of corresponding genes. The log2 of the gene expression levels (FPKM) was calculated and is presented. The red and blue curves in each plot represent gene expression levels and non-CpG DNA methylation levels in gene body regions, respectively.

Supplementary Figure S4. DNA methylation changes of DMRs of bovine gametes during preimplantation development. (a and b) Histogrm plots of DNA methylation levels for hypermethylated and hypomethylated 100-bp tiles in sperm and in vitro matured oocytes across early embryonic development stages. (c and d) Histogram plots of DNA methylation levels for hypermethylated and hypomethylated 100-bp tiles in sperm and GV oocytes across early embryonic development stages. (e) Heatmap of the methylation level of sperm-specific DMRs between sperm and GV oocytes among different genomic regions across different developmental stages. (f) Heatmap of the methylation level of in vivo MII oocyte-specific DMRs between sperm and GV oocytes among different genomic regions across different developmental stages. (g) Box plots of DNA methylation levels of sperm-specific DMRs between sperm and in vitro matured oocytes across early embryonic development stages. (h) Box plots of DNA methylation levels of in vivo derived MII oocyte-specific DMRs between sperm and in vitro matured oocytes across early embryonic development stages. (i) Box plots of DNA methylation levels of sperm-specific DMRs between sperm and GV oocytes across early embryonic development stages. (j) Box plots of DNA methylation levels of in vitro matured oocyte-specific DMRs in comparisons between sperm and in vitro matured oocytes across early embryonic development stages. (k) Heatmap of the methylation level of sperm-specific DMRs in comparisons between sperm and in vitro matured oocytes among different genomic regions across different developmental stages. (**l**) Heatmap of the methylation level of in vitro MII oocyte-specific DMRs in comparisons between sperm and in vitro matured oocytes among different genomic regions across different developmental stages. In each of these panels, the color keys from green to red indicate methylation levels from low to high.

Supplementary Figure S5. (a) Dynamics of DNA methylation of LINEs (L1, L2, and BovB) during bovine embryo development. (**b**) Expression patterns of LINEs (L1, L2, and BovB) during bovine embryo development.

Supplementary Table S1. Summary of the sequencing qualities, read mapping, the average covered CpG sites at 1X, 5X, and 10X, and the bisulfite conversion rate in each stage of the bovine early development.

Supplementary Table S2. List of the top 20 genes whose promoter methylation was significantly and inversely correlated with gene expression at the 8-cell stage.

Supplementary Table S3. The hypergeometric enrichment analysis of the hypermethylated and hypomethylated tiles in bovine gametes exhibited the strong enrichment for different genomic regions (hypergometric enrichment test).

Supplementary Table S4. Methylation levels of DMRs in sperm and in vivo_MII oocytes. Tiles that were highly methylated in sperm (**3a**) and oocytes (**3b**) are shown.

Supplementary Table S5. Methylation levels of DMRs in in vivo_MII and In vitro_MII oocytes. Tiles that were highly methylated in In vitro_MII oocytes (**4a**) and In vivo_MII oocytes (**3b**) are shown.

Acknowledgements

We thank Yang Zhou and George Liu for suggestions on bovine transposable element annotation and analysis. This project was supported by grants from the USDA (1265-31000-091-02S and W2171/3171) and National Natural Science Foundation of China (30760167). Ouyang lab was supported by the National Institute of General Medical Sciences (NIGMS) of the National Institutes of Health under award number R35GM124998 and The Jackson Laboratory for Genomic Medicine faculty start-up fund.

Authors' contributions: XCT and ZJ conceived the study; HD, XZ and JC collected samples and ZJ performed all the experiments; JL, performed data analysis with assistance from ZJ, SLM, JD, and XCT; ZO supervised data analysis; ZJ, SLM, and XCT interpreted the data and wrote the manuscript with help from all of the authors. All authors read and approved the final manuscript.

Conflict of Interest: The authors have declared that no conflict of interest.

References

1. Bird A. DNA methylation patterns and epigenetic memory. *Genes Dev* 2002; **16**:6–21.
2. Jaenisch R, Bird A. Epigenetic regulation of gene expression: how the genome integrates intrinsic and environmental signals. *Nat Genet* 2003; **33**:245–254.
3. Li E, Beard C, Jaenisch R. Role for DNA methylation in genomic imprinting. *Nature* 1993; **366**:362–365.
4. Smallwood SA, Tomizawa S, Krueger F, Ruf N, Carli N, Segonds-Pichon A, Sato S, Hata K, Andrews SR, Kelsey G. Dynamic CpG island methylation landscape in oocytes and preimplantation embryos. *Nat Genet* 2011; **43**:811–814.
5. Seisenberger S, Andrews S, Krueger F, Arand J, Walter J, Santos F, Popp C, Thienpont B, Dean W, Reik W. The dynamics of genome-wide DNA methylation reprogramming in mouse primordial germ cells. *Mol Cell* 2012; **48**:849–862.
6. Smith ZD, Chan MM, Mikkelsen TS, Gu H, Gnirke A, Regev A, Meissner A. A unique regulatory phase of DNA methylation in the early mammalian embryo. *Nature* 2012; **484**:339–344.
7. Guo H, Zhu P, Yan L, Li R, Hu B, Lian Y, Yan J, Ren X, Lin S, Li J, Jin X, Shi X et al. The DNA methylation landscape of human early embryos. *Nature* 2014; **511**:606–610.
8. Smith ZD, Chan MM, Humm KC, Karnik R, Mekhoubad S, Regev A, Eggan K, Meissner A. DNA methylation dynamics of the human preimplantation embryo. *Nature* 2014; **511**:611–615.
9. Gkountela S, Zhang KX, Shafiq TA, Liao WW, Hargan-Calvopina J, Chen PY, Clark AT. DNA Demethylation dynamics in the human prenatal germline. *Cell* 2015; **161**:1425–1436.
10. Guo F, Yan L, Guo H, Li L, Hu B, Zhao Y, Yong J, Hu Y, Wang X, Wei Y, Wang W, Li R et al. The transcriptome and DNA methylome landscapes of human primordial germ cells. *Cell* 2015; **161**:1437–1452.
11. Gao F, Niu YY, Sun YE, Lu HL, Chen YC, Li SG, Kang Y, Luo YP, Si CY, Yu JH, Li C, Sun NQ et al. De novo DNA methylation during monkey pre-implantation embryogenesis. *Cell Res* 2017; **27**:526–539.
12. Inoue A, Zhang Y. Replication-dependent loss of 5-hydroxymethylcytosine in mouse preimplantation embryos. *Science* 2011; **334**:194–194.
13. Iqbal K, Jin SG, Pfeifer GP, Szabo PE. Reprogramming of the paternal genome upon fertilization involves genome-wide oxidation of 5-methylcytosine. *Proc Natl Acad Sci USA* 2011; **108**:3642–3647.
14. Wossidlo M, Nakamura T, Lepikhov K, Marques CJ, Zakhartchenko V, Boiani M, Arand J, Nakano T, Reik W, Walter J. 5-Hydroxymethylcytosine in the mammalian zygote is linked with epigenetic reprogramming. *Nat Commun* 2011; **2**:241.
15. Nakamura T, Arai Y, Umehara H, Masuhara M, Kimura T, Taniguchi H, Sekimoto T, Ikawa M, Yoneda Y, Okabe M, Tanaka S, Shiota K et al. PGC7/Stella protects against DNA demethylation in early embryogenesis. *Nat Cell Biol* 2007; **9**:64–71.
16. Nakamura T, Liu YJ, Nakashima H, Umehara H, Inoue K, Matoba S, Tachibana M, Ogura A, Shinkai Y, Nakano T. PGC7 binds histone H3K9me2 to protect against conversion of 5mC to 5hmC in early embryos. *Nature* 2012; **486**:415–419.
17. Bakhtari A, Ross PJ. DPPA3 prevents cytosine hydroxymethylation of the maternal pronucleus and is required for normal development in bovine embryos. *Epigenetics* 2014; **9**:1271–1279.
18. Dean W, Santos F, Stojkovic M, Zakhartchenko V, Walter J, Wolf E, Reik W. Conservation of methylation reprogramming in mammalian development: aberrant reprogramming in cloned embryos. *Proc Natl Acad Sci USA* 2001; **98**:13734–13738.
19. Santos F, Hendrich B, Reik W, Dean W. Dynamic reprogramming of DNA methylation in the early mouse embryo. *Dev Biol* 2002; **241**:172–182.
20. Petrussa L, Van de Velde H, De Rycke M. Similar kinetics for 5-methylcytosine and 5-hydroxymethylcytosine during human preimplantation development in vitro. *Mol Reprod Dev* 2016; **83**:594–605.
21. Dobbs KB, Rodriguez M, Sudano MJ, Ortega MS, Hansen PJ. Dynamics of DNA methylation during early development of the preimplantation bovine embryo. *PLoS One* 2013; **8**:e66230.
22. Zhang S, Chen X, Wang F, An X, Tang B, Zhang X, Sun L, Li Z. Aberrant DNA methylation reprogramming in bovine SCNT preimplantation embryos. *Sci Rep* 2016; **6**:30345.
23. Salilew-Wondim D, Fournier E, Hoelker M, Saeed-Zidane M, Tholen E, Looft C, Neuhoff C, Besenfelder U, Havlicek V, Rings F, Gagne D, Sirard MA et al. Genome-Wide DNA methylation patterns of bovine blastocysts developed in vivo from embryos completed different stages of development in vitro. *PLoS One* 2015; **10**:e0140467.
24. O'Doherty AM, Magee DA, O'Shea LC, Forde N, Beltman ME, Mamo S, Fair T. DNA methylation dynamics at imprinted genes during bovine pre-implantation embryo development. *BMC Dev Biol* 2015; **15**:13.
25. Mattern F, Herrmann D, Heinzmann J, Hadeler KG, Bernal-Ulloa SM, Haaf T, Niemann H. DNA methylation and mRNA expression of developmentally important genes in bovine oocytes collected from donors of different age categories. *Mol Reprod Dev* 2016; **83**:802–814.
26. Urrego R, Bernal-Ulloa SM, Chavarria NA, Herrera-Puerta E, Lucas-Hahn A, Herrmann D, Winkler S, Pache D, Niemann H, Rodriguez-Osorio N. Satellite DNA methylation status and expression of selected genes in Bos indicus blastocysts produced in vivo and in vitro. *Zygote* 2017; **25**:131–140.
27. Li T, Vu TH, Ulaner GA, Littman E, Ling JQ, Chen HL, Hu JF, Behr B, Giudice L, Hoffman AR. IVF results in de novo DNA methylation and histone methylation at an Igf2-H19 imprinting epigenetic switch. *Mol Hum Reprod* 2005; **11**:631–640.
28. Fernandez-Gonzalez R, Ramirez MA, Pericuesta E, Calle A, Gutierrez-Adan A. Histone modifications at the blastocyst Axin1Fu locus mark the heritability of in vitro Culture-Induced epigenetic alterations in Mice1. *Biol Reprod* 2010; **83**:720–727.
29. Sutcliffe AG, Peters CJ, Bowdin S, Temple K, Reardon W, Wilson L, Clayton-Smith J, Brueton LA, Bannister W, Maher ER. Assisted reproductive therapies and imprinting disorders–a preliminary British survey. *Hum Reprod* 2006; **21**:1009–1011.
30. Young LE, Sinclair KD, Wilmut I. Large offspring syndrome in cattle and sheep. *Rev Reprod* 1998; **3**:155–163.
31. Chen Z, Robbins KM, Wells KD, Rivera RM. Large offspring syndrome. *Epigenetics* 2013; **8**:591–601.
32. Rizos D, Ward F, Duffy P, Boland MP, Lonergan P. Consequences of bovine oocyte maturation, fertilization or early embryo development in vitro versus in vivo: implications for blastocyst yield and blastocyst quality. *Mol Reprod Dev* 2002; **61**:234–248.
33. Jiang Z, Sun J, Dong H, Luo O, Zheng X, Obergfell C, Tang Y, Bi J, O'Neill R, Ruan Y, Chen J, Tian XC. Transcriptional profiles of bovine in vivo pre-implantation development. *BMC Genomics* 2014; **15**:756.
34. Guo H, Zhu P, Guo F, Li X, Wu X, Fan X, Wen L, Tang F. Profiling DNA methylome landscapes of mammalian cells with single-cell reduced-representation bisulfite sequencing. *Nat Protoc* 2015; **10**:645–659.
35. Krueger F, Andrews SR. Bismark: a flexible aligner and methylation caller for Bisulfite-Seq applications. *Bioinformatics* 2011; **27**:1571–1572.
36. Huang da W, Sherman BT, Lempicki RA. Systematic and integrative analysis of large gene lists using DAVID bioinformatics resources. *Nat Protoc* 2009; **4**:44–57.
37. Graf A, Krebs S, Zakhartchenko V, Schwalb B, Blum H, Wolf E. Fine mapping of genome activation in bovine embryos by RNA sequencing. *Proc Natl Acad Sci USA* 2014; **111**:4139–4144.
38. Kim D, Pertea G, Trapnell C, Pimentel H, Kelley R, Salzberg SL. TopHat2: accurate alignment of transcriptomes in the presence of insertions, deletions and gene fusions. *Genome Biol* 2013; **14**:R36.
39. Trapnell C, Roberts A, Goff L, Pertea G, Kim D, Kelley DR, Pimentel H, Salzberg SL, Rinn JL, Pachter L. Differential gene and transcript expression analysis of RNA-seq experiments with TopHat and Cufflinks. *Nat Protoc* 2012; **7**:562–578.
40. Wang L, Zhang J, Duan J, Gao X, Zhu W, Lu X, Yang L, Zhang J, Li G, Ci W, Li W, Zhou Q et al. Programming and inheritance of parental DNA methylomes in mammals. *Cell* 2014; **157**:979–991.
41. Fulka H, Mrazek M, Tepla O, Fulka J, Jr. DNA methylation pattern in human zygotes and developing embryos. *Reproduction* 2004; **128**:703–708.

42. Reis e Silva AR, Bruno C, Fleurot R, Daniel N, Archilla C, Peynot N, Lucci CM, Beaujean N, Duranthon V. Alteration of DNA demethylation dynamics by in vitro culture conditions in rabbit pre-implantation embryos. *Epigenetics* 2012; **7**:440–446.
43. Canovas S, Ross PJ, Kelsey G, Coy P. DNA Methylation in embryo development: epigenetic impact of ART (Assisted Reproductive Technologies). *Bioessays* 2017 Nov; **39**(11).
44. Salvaing J, Li Y, Beaujean N, O'Neill C. Determinants of valid measurements of global changes in 5′-methylcytosine and 5′-hydroxymethylcytosine by immunolocalisation in the early embryo. *Reprod Fertil Dev* 2015; **27**:755–764.
45. Okae H, Chiba H, Hiura H, Hamada H, Sato A, Utsunomiya T, Kikuchi H, Yoshida H, Tanaka A, Suyama M, Arima T. Genome-wide analysis of DNA methylation dynamics during early human development. *PLoS Genet* 2014; **10**:e1004868.
46. Misirlioglu M, Page GP, Sagirkaya H, Kaya A, Parrish JJ, First NL, Memili E. Dynamics of global transcriptome in bovine matured oocytes and preimplantation embryos. *Proc Natl Acad Sci USA* 2006; **103**:18905–18910.
47. Kues WA, Sudheer S, Herrmann D, Carnwath JW, Havlicek V, Besenfelder U, Lehrach H, Adjaye J, Niemann H. Genome-wide expression profiling reveals distinct clusters of transcriptional regulation during bovine preimplantation development in vivo. *Proc Natl Acad Sci USA* 2008; **105**:19768–19773.
48. Kurihara Y, Kawamura Y, Uchijima Y, Amamo T, Kobayashi H, Asano T, Kurihara H. Maintenance of genomic methylation patterns during preimplantation development requires the somatic form of DNA methyltransferase 1. *Dev Biol* 2008; **313**:335–346.
49. Braude P, Bolton V, Moore S. Human gene expression first occurs between the four- and eight-cell stages of preimplantation development. *Nature* 1988; **332**:459–461.
50. Hamatani T, Carter MG, Sharov AA, Ko MS. Dynamics of global gene expression changes during mouse preimplantation development. *Dev Cell* 2004; **6**:117–131.
51. Wang QT, Piotrowska K, Ciemerych MA, Milenkovic L, Scott MP, Davis RW, Zernicka-Goetz M. A genome-wide study of gene activity reveals developmental signaling pathways in the preimplantation mouse embryo. *Dev Cell* 2004; **6**:133–144.
52. Yan L, Yang M, Guo H, Yang L, Wu J, Li R, Liu P, Lian Y, Zheng X, Yan J, Huang J, Li M et al. Single-cell RNA-Seq profiling of human preimplantation embryos and embryonic stem cells. *Nat Struct Mol Biol* 2013; **20**:1131–1139.
53. Niwa H, Toyooka Y, Shimosato D, Strumpf D, Takahashi K, Yagi R, Rossant J. Interaction between Oct3/4 and Cdx2 determines trophectoderm differentiation. *Cell* 2005; **123**:917–929.
54. Strumpf D, Mao CA, Yamanaka Y, Ralston A, Chawengsaksophak K, Beck F, Rossant J. Cdx2 is required for correct cell fate specification and differentiation of trophectoderm in the mouse blastocyst. *Development* 2005; **132**:2093–2102.
55. Sakurai N, Takahashi K, Emura N, Fujii T, Hirayama H, Kageyama S, Hashizume T, Sawai K. The necessity of OCT-4 and CDX2 for early development and gene expression involved in differentiation of inner cell mass and trophectoderm lineages in bovine embryos. *Cell Reprogram* 2016; **18**:309–318.
56. Watson AJ. Oocyte cytoplasmic maturation: A key mediator of oocyte and embryo developmental competence1. *J Anim Sci* 2007; **85**:E1–E3.
57. Smith SL, Everts RE, Sung LY, Du F, Page RL, Henderson B, Rodriguez-Zas SL, Nedambale TL, Renard JP, Lewin HA, Yang X, Tian XC. Gene expression profiling of single bovine embryos uncovers significant effects of in vitro maturation, fertilization and culture. *Mol Reprod Dev* 2009; **76**:38–47.
58. Tomizawa S, Kobayashi H, Watanabe T, Andrews S, Hata K, Kelsey G, Sasaki H. Dynamic stage-specific changes in imprinted differentially methylated regions during early mammalian development and prevalence of non-CpG methylation in oocytes. *Development* 2011; **138**:811–820.
59. Shirane K, Toh H, Kobayashi H, Miura F, Chiba H, Ito T, Kono T, Sasaki H. Mouse oocyte methylomes at base resolution reveal genome-wide accumulation of non-CpG methylation and role of DNA methyltransferases. *PLoS Genet* 2013; **9**:e1003439.
60. Lister R, Pelizzola M, Dowen RH, Hawkins RD, Hon G, Tonti-Filippini J, Nery JR, Lee L, Ye Z, Ngo QM, Edsall L, Antosiewicz-Bourget J et al. Human DNA methylomes at base resolution show widespread epigenomic differences. *Nature* 2009; **462**:315–322.
61. Barres R, Kirchner H, Rasmussen M, Yan J, Kantor FR, Krook A, Naslund E, Zierath JR. Weight loss after gastric bypass surgery in human obesity remodels promoter methylation. *Cell Rep* 2013; **3**:1020–1027.
62. Barres R, Osler ME, Yan J, Rune A, Fritz T, Caidahl K, Krook A, Zierath JR. Non-CpG methylation of the PGC-1alpha promoter through DNMT3B controls mitochondrial density. *Cell Metab* 2009; **10**:189–198.
63. Patil V, Ward RL, Hesson LB. The evidence for functional non-CpG methylation in mammalian cells. *Epigenetics* 2014; **9**:823–828.
64. Smith ZD, Meissner A. DNA methylation: roles in mammalian development. *Nat Rev Genet* 2013; **14**:204–220.
65. Okano M, Bell DW, Haber DA, Li E. DNA methyltransferases Dnmt3a and Dnmt3b are essential for de novo methylation and mammalian development. *Cell* 1999; **99**:247–257.
66. Sela N, Kim E, Ast G. The role of transposable elements in the evolution of non-mammalian vertebrates and invertebrates. *Genome Biol* 2010; **11**:R59.
67. Lev Maor G, Yearim A, Ast G. The alternative role of DNA methylation in splicing regulation. *Trends Genet* 2015; **31**:274–280.
68. Leibfried-Rutledge ML, Critser ES, Eyestone WH, Northey DL, First NL. Development potential of bovine oocytes matured in vitro or in vivo. *Biol Reprod* 1987; **36**:376–383.
69. Adelson DL, Raison JM, Edgar RC. Characterization and distribution of retrotransposons and simple sequence repeats in the bovine genome. *Proc Natl Acad Sci USA* 2009; **106**:12855–12860.
70. Li Y, Sasaki H. Genomic imprinting in mammals: its life cycle, molecular mechanisms and reprogramming. *Cell Res* 2011; **21**:466–473.
71. O'Doherty AM, O'Shea LC, Fair T. Bovine DNA methylation imprints are established in an oocyte size-specific manner, which are coordinated with the expression of the DNMT3 family proteins. *Biol Reprod* 2012; **86**:67.
72. Gebert C, Wrenzycki C, Herrmann D, Groger D, Reinhardt R, Hajkova P, Lucas-Hahn A, Carnwath J, Lehrach H, Niemann H. The bovine IGF2 gene is differentially methylated in oocyte and sperm DNA. *Genomics* 2006; **88**:222–229.
73. Gebert C, Wrenzycki C, Herrmann D, Groger D, Thiel J, Reinhardt R, Lehrach H, Hajkova P, Lucas-Hahn A, Carnwath JW, Niemann H. DNA methylation in the IGF2 intragenic DMR is re-established in a sex-specific manner in bovine blastocysts after somatic cloning. *Genomics* 2009; **94**:63–69.
74. Tian XC. Genomic imprinting in farm animals. *Annu Rev Anim Biosci* 2014; **2**:23–40.
75. Chen Z, Hagen DE, Elsik CG, Ji T, Morris CJ, Moon LE, Rivera RM. Characterization of global loss of imprinting in fetal overgrowth syndrome induced by assisted reproduction. *Proc Natl Acad Sci USA* 2015; **112**:4618–4623.
76. Jiang ZL, Dong H, Zheng XB, Marjani SL, Donovan DM, Chen JB, Tian XC. mRNA levels of imprinted genes in bovine in vivo oocytes, embryos and cross species comparisons with humans, mice and pigs. *Sci Rep* 2015; **5**:17898.
77. Lucifero D, Suzuki J, Bordignon V, Martel J, Vigneault C, Therrien J, Filion F, Smith LC, Trasler JM. Bovine SNRPN methylation imprint in oocytes and day 17 in Vitro-Produced and somatic cell nuclear transfer embryos. *Biol Reprod* 2006; **75**:531–538.
78. Bartolomei MS. Genomic imprinting: employing and avoiding epigenetic processes. *Genes Dev* 2009; **23**:2124–2133.
79. Wan LB, Bartolomei MS. Regulation of imprinting in clusters: noncoding RNAs versus insulators. *Adv Genet* 2008; **61**:207–223.
80. Barlow DP, Bartolomei MS. Genomic imprinting in mammals. *Cold Spring Harb Perspect Biol* 2014; **6**:a01838.
81. Bartolomei MS, Ferguson-Smith AC. Mammalian genomic imprinting. *Cold Spring Harb Perspect Biol* 2011; **3**:a002592.